

Experiment towards continuous variable entanglement swapping: Highly correlated four-partite quantum state

Oliver Glöckl^{1,*}, Stefan Lorenz¹, Christoph Marquardt¹, Joel Heersink¹, Michael Brownnutt¹, Christine Silberhorn¹, Qing Pan^{1,2}, Peter van Loock¹, Natalia Korolkova¹, and Gerd Leuchs¹

¹Zentrum für Moderne Optik, Physikalisches Institut,

Universität Erlangen-Nürnberg, Staudtstraße 7/B2, 91058 Erlangen, Germany

²The State Key Laboratory of Quantum Optics and Quantum Optics Devices,

Institute of Opto-Electronics, Shanxi University, Taiyuan, 030006, P.R.China

(Dated: October 29, 2018)

We present a protocol for performing entanglement swapping with intense pulsed beams. In a first step, the generation of amplitude correlations between two systems that have never interacted directly is demonstrated. This is verified in direct detection with electronic modulation of the detected photocurrents. The measured correlations are better than expected from a classical reconstruction scheme. In an entanglement swapping process, a four-partite entangled state is generated. We prove experimentally that the amplitudes of the four optical modes are quantum correlated 3 dB below shot noise, which is consistent with the presence of genuine four-party entanglement.

PACS numbers: 03.67.Hk, 42.50.Dv, 42.65.Tg

I. INTRODUCTION

Entanglement is the basic resource for quantum information applications. We are dealing with intense, pulsed light which is described by continuous quantum variables and which allows for efficient detection schemes and reliable sources. The generation of entanglement shared by two parties is now achieved routinely in the laboratories, e. g. entanglement of the quadrature components of an electromagnetic field. These two party entangled states may enhance the capability of the two parties to communicate. There are already several experimental realisations of quantum information and quantum communication protocols over continuous variables, exploiting entanglement, for example, quantum dense coding [1] and quantum teleportation [2].

Initially, quantum communication dealt almost exclusively with discrete two-valued quantum variables. The first demonstration of teleportation, i. e. the transfer of a quantum state from one party to another was reported by Bouwmeester et al. [3]. The scheme was close to the theoretical proposal by Bennett et al. [4]. In the experiment, the polarization state of a single photon was teleported using a pair of polarization entangled photons. However, the experiment was not an unconditional teleportation, as only one of the four possible results of the Bell-state measurement can be discriminated against the others. As a next step, quantum entanglement swapping, i. e. the teleportation of entanglement, was demonstrated experimentally by Pan et al. [5]. More recently, unconditional teleportation of an unknown polarization state was demonstrated by Kim et al. [6], employing nonlinear interactions to discriminate the entire set of Bell-states, however at low efficiency. These initial experiments relied

upon the polarization of a single photon to encode the qubit. Recently, long distance teleportation was demonstrated by encoding the qubit into the superposition of a single photon in two different locations (time bins) [7]. In all these experiments, discrete quantum variables were teleported.

For continuous variables, such as the amplitude and the phase quadratures of an electromagnetic field, which are used in this paper, only the quantum teleportation of coherent states has been demonstrated so far. The first experiment was reported by Furusawa et al. [2] and was based on a proposal by Braunstein and Kimble [8]. The advantage of this experiment is that unconditional teleportation was demonstrated, i. e. no postselection of successful events was necessary. However, the quality of the teleportation, i. e. the fidelity is limited by the quality of the correlations of the auxiliary entangled beam pair. In that first experiment the fidelity was 0.58. Recently, there have been reports on further improvements in teleportation experiments of coherent states, with fidelities of 0.62 [9] and 0.64 [10].

So far, no entanglement swapping with continuous variables has been reported. However, entanglement swapping is interesting for several reasons: First, among all quantum states of the light field coherent states are closest to classical states while entanglement swapping refers to the teleportation of a highly non-classical state. Second, the success of entanglement swapping can be checked easily by verifying the correlations generated in the entanglement swapping process. In general, for more complex applications towards quantum networking it is desirable to achieve entanglement swapping combined with entanglement purification [11], as it enables the distribution of entanglement and non-classical correlations over large distances between systems that have never interacted directly.

Multipartite entanglement, the entanglement shared by more than two parties, is also a useful resource for

*Electronic address: gloeckl@kerr.physik.uni-erlangen.de

quantum networking. For example, the distribution of quantum information to several receivers, called telecloning [12] or for quantum secret sharing [13] are based on multi-party entangled states.

In this paper, we present our work towards entanglement swapping using intense beams. We present a possible entanglement swapping scheme and describe and characterize our entanglement sources. For entanglement swapping, two independent EPR-sources are needed which are then made to interfere. By a direct analysis of the detected photocurrents we prove that strong correlations are created between the amplitude quadratures in the entanglement swapping process. This experiment is a first step towards the teleportation of a highly non-classical state. We also show that with the same basic resource, i. e. the coupling of two entanglement sources, a highly correlated four-party state is generated. A preliminary theoretical analysis, neglecting the excess thermal phase noise in the EPR-sources and hence assuming them to be pure, indicates that the generated state is indeed a genuinely four-party entangled state.

II. ENTANGLEMENT SWAPPING PROTOCOL

The scheme for entanglement swapping is outlined in Fig. 1. Two pairs of quadrature entangled beams denoted EPR I and EPR II are generated by linear interference of two amplitude squeezed beams. Initially, the beam pair labelled EPR1 and EPR2 and the one labelled EPR3 and EPR4 are two independent entangled pairs. The experiment aims at achieving entanglement between the beams 1 and 4. This requires the teleportation of beam EPR2 to the output mode EPR4 and is referred to as entanglement swapping. For that purpose, one beam from each entanglement source, i. e. EPR-beam 2 and EPR-beam 3 are combined at a 50/50 beam splitter with the phase φ_3 adjusted such that the two output beams are equally intense (Fig. 1). The resulting beams are denoted Mode5 and Mode6.

The Bell-state measurement is completed by the joint detection of Mode5 and Mode6 (see Fig. 1). The signals obtained from that measurement are used to modulate the amplitude and the phase of EPR4 to yield OUT2, which in the ideal case should now be a copy of the mode EPR2 and show strong non-classical correlations with EPR1, now called OUT1. The signals needed for the modulation are described by $(\delta\hat{X}_5 + \delta\hat{X}_6)$ and $(\delta\hat{Y}_5 - \delta\hat{Y}_6)$, where $\delta\hat{X}$ and $\delta\hat{Y}$ denote the fluctuations in the amplitude and the phase quadrature. The quadrature components [14] of the electromagnetic field are defined by $\hat{X} = \hat{a}^\dagger + \hat{a}$ and $\hat{Y} = i(\hat{a}^\dagger - \hat{a})$. The sum- and difference variances can be obtained in direct detection without local oscillator techniques, provided the measurement is performed on intense beams [15–17]. In a next step, the fluctuating results of the photon number measurements on Mode5 and Mode6, $\delta\hat{n}_5$ and $\delta\hat{n}_6$ are detected. Taking simultaneously the sum and the difference

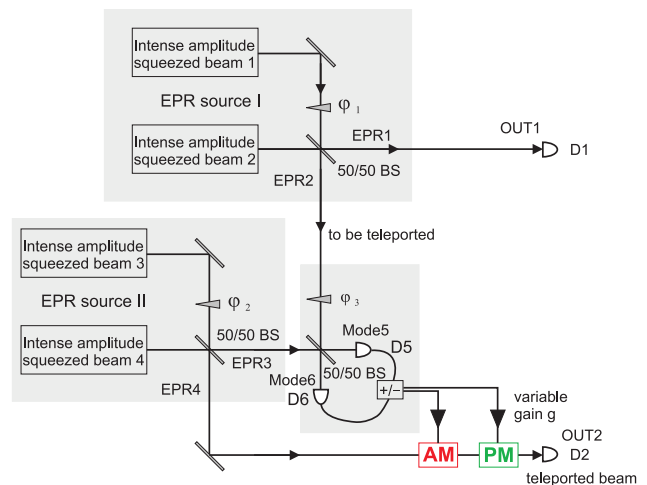


FIG. 1: Schematic drawing of the entanglement swapping experiment

of the corresponding photocurrents, that is $\delta\hat{n}_5 + \delta\hat{n}_6$ and $\delta\hat{n}_5 - \delta\hat{n}_6$, signals are obtained which are proportional to the sum and difference quadratures mentioned above. The corresponding photocurrents which are transmitted over the classical channel to the modulators are denoted $i_{\text{Bell}}^+ = i5 + i6$ and $i_{\text{Bell}}^- = i5 - i6$, respectively.

An optimum gain g for the modulation can be chosen such that after the entanglement swapping process the highest possible correlations between the output beams OUT1 and OUT2 are generated. The gain g describes to what degree initial fluctuations of one beam are transferred onto an output mode after detection of the initial mode and subsequent modulation of the output mode with that signal. In the case of infinite input squeezing $g = 1$ is optimal, while for finite squeezing values of $g < 1$ are better. The value of g also depends on the degree of excess noise in the anti-squeezed quadrature, i. e. the optimum value for g is different for non-minimum uncertainty squeezed states and for minimum uncertainty states. The optimum value for g has to be chosen closer to one the more excess phase noise is present.

It was shown [18] that for any finitely squeezed minimum uncertainty vacuum states, EPR-correlations between the output modes OUT1 and OUT2 can always be generated independent of the degree of input squeezing using an optimized gain. This also holds true for intense squeezed beams that we employ in our experiment. However, for states with high excess noise in the phase quadrature, say about 20dB as in our experiment, the optimum gain is close to $g = 1$. Hence there is a 3dB penalty in the correlations created between the output states. Therefore, in this case, the generation of non-classical EPR-correlations in the entanglement swapping process requires more than 3dB initial squeezing.

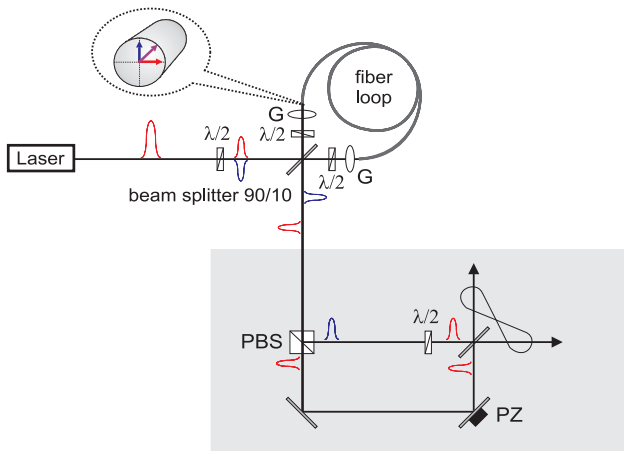


FIG. 2: Generation of squeezing using an asymmetric fiber Sagnac interferometer. $\lambda/2$: half wave plate, G: gradient index lens, PBS: polarizing beam splitter, PZ: piezo actuator. Two independently squeezed modes are generated as the light propagates on both optical axes of the optical fiber. The gray shaded area shows the interference of both amplitude squeezed fields to generate entanglement.

III. EXPERIMENTAL SETUP AND MEASUREMENT RESULTS

A. Entanglement source

The intense squeezed beams are generated using an asymmetric fiber Sagnac interferometer, exploiting the Kerr nonlinearity. The setup is depicted in Fig. 2.

In the asymmetric fiber Sagnac interferometer, two counter propagating pulses, one strong pulse and one weak pulse, are coupled into a polarization maintaining fiber. Due to the Kerr nonlinearity, the strong pulse acquires an intensity dependent phase shift, while the weak pulse is largely unaffected by nonlinear effects. Thus, the initially circular shaped uncertainty area in phase space is transformed into an ellipse. By interference with the weak pulse, the uncertainty ellipse is reoriented in phase space, resulting in direct detectable amplitude squeezing [19]. Choosing an input polarization of about 45° with respect to the optical axes of the fiber, two independently squeezed beams in s- and in p-polarization can be generated simultaneously [20, 21]. In the following this interferometer is referred to as a double squeezer.

Quadrature entanglement is generated by linear interference of two amplitude squeezed fields with proper phase relation [16, 21]. Due to the birefringence of the fiber, the relative delay of the pulses has to be compensated before they are combined on a 50/50 beam splitter to generate entanglement (see the shaded region in Fig. 2). The EPR-entanglement is maximized when the interference phase is such that the two output beams have equal optical power. An active feedback control to stabilize the interference phase is used.

The entanglement is characterized in terms of the non-

separability criterion for two mode Gaussian states [22, 23]. The non-separability criterion can be expressed in terms of observable quantities, the so called squeezing variances [24]:

$$V_{\text{sq}}^{\pm}(\delta\hat{X}) = \frac{V(\delta\hat{X}_i \pm g\delta\hat{X}_j)}{V(\delta\hat{X}_{i,\text{coh}} + g\delta\hat{X}_{j,\text{coh}})}, \quad (1)$$

$$V_{\text{sq}}^{\mp}(\delta\hat{Y}) = \frac{V(\delta\hat{Y}_i \mp g\delta\hat{Y}_j)}{V(\delta\hat{Y}_{i,\text{coh}} + g\delta\hat{Y}_{j,\text{coh}})} \quad (2)$$

where $V(\hat{A}) = \langle \hat{A}^2 \rangle - \langle \hat{A} \rangle^2$ denotes the variance of an operator \hat{A} and $i \neq j$ and g is a variable gain. The quadrature components labelled with index ‘‘coh’’ are those of a coherent state. The non-separability criterion then reads [24]:

$$V_{\text{sq}}^{\pm}(\delta\hat{X}) + V_{\text{sq}}^{\mp}(\delta\hat{Y}) < 2. \quad (3)$$

B. Towards entanglement swapping—direct analysis of the photocurrent

In this section we describe a scheme that permits us to check for correlations in the amplitude quadrature created by the entanglement swapping process by direct analysis of the photocurrents. The signal from the Bell-measurement, i_{Bell}^+ , that will be used for the modulation is a classical signal. If the emerging entangled pair, OUT1 and OUT2, were to be used as a quantum resource, the signal from the Bell-state measurement has to be used to modulate the optical mode EPR4 (see Fig. 1). However, if the mode OUT2 is just detected to verify the success of entanglement swapping, modulation of EPR4 can be substituted by direct summation of the photocurrents. Thus, the measured photocurrents are identical in the case of optical modulation of EPR4 and detecting OUT2 and in the case of measuring EPR4 and adding the photocurrent i_{Bell}^+ , giving $i4 + i_{\text{Bell}}^+$ (see Fig. 3). In this context, we performed the following experiment towards entanglement swapping as it is depicted in Fig. 3.

Two entanglement sources were set up, each consisted of a double squeezer and a subsequent interferometer to generate entanglement. In each squeezer, 8m of polarization maintaining fiber (FS-PM-7811 from 3M) was used, the splitting ratio of the asymmetric beam splitter was 90/10. The laser source used in the experiment is a commercially available OPO (OPAL from Spectra Physics) pumped by a mode locked Ti:Sapphire laser (Tsunami from Spectra Physics). It produces pulses of 100fs at a center wavelength of 1530nm and a repetition rate of 82MHz. Squeezing was produced at an output pulse energy of about 27pJ for each polarization.

Each squeezer produced more than 3dB amplitude squeezed light in each polarization. This results in squeezing variances of 3dB for both entanglement sources (see Fig. 4). The degree of correlations was measured for the amplitude quadrature, but due to the symmetry of

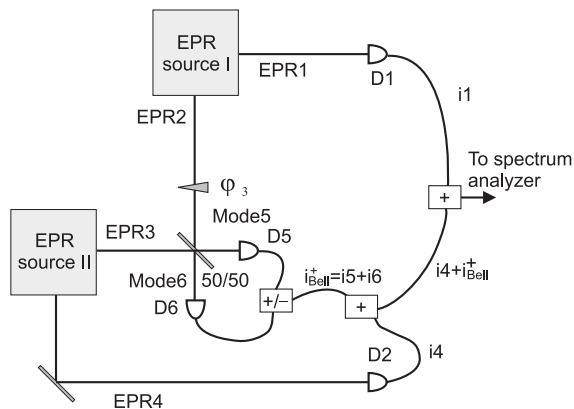


FIG. 3: Entanglement swapping, direct analysis of the photocurrents

the generation process, the squeezing variances $V_{\text{sq}}^+(\delta\hat{X})$ and $V_{\text{sq}}^-(\delta\hat{Y})$ for the amplitude and phase quadrature should be the same. The peaks in the noise measurement of the entanglement source II are due to instabilities of the laser power. The corresponding shot noise levels were obtained by measuring the noise power when the detectors were illuminated with coherent light of the same classical field amplitude as that of the squeezed states. The shot noise was calibrated by illuminating the detectors with coherent light. This calibration was checked before the experiment by comparing the measured noise level of a coherent beam with the shot noise level determined by the difference signal of a balanced detection setup. In the following, none of the measured noise traces was corrected for the electronic noise which was at -87.8dBm .

The next step is the interference between the two independently generated EPR-beams 2 and 3. The interference is a critical part of the experiment, since a good spectral, temporal and spatial overlap of the interfering modes is required. Therefore it is important that the beams have propagated through the same fiber length. Moreover, both squeezers were prepared with fiber pieces from the same coil. Still, the fiber pieces are not identical, therefore the pulses from the different squeezers acquire different phase noise, which might be due to different contributions from guided acoustic wave Brillouin scattering (GAWBS) in different fiber pieces. Nevertheless it was possible to achieve a visibility of up to 85% and to stabilize the interference phase between EPR2 and EPR3, so that the two output modes are equally intense. This is worth noting, as we have achieved interference between two modes of independently generated entangled systems.

Four photodetectors were placed in the four output modes of the setup, i.e. EPR1, EPR4, Mode5, and Mode6. Each of the detectors used a high efficiency InGaAs-photodiode (Epitaxx ETX 500). To avoid saturation of the detectors, a Chebycheff lowpass filter was used with a cutoff frequency of about 35MHz to suppress

the high noise peaks at the repetition frequency and the harmonics of the laser. The photocurrent fluctuations were detected at a frequency of 17.5MHz with a resolution bandwidth of 300kHz. The measurements were averaged with a video bandwidth of 30Hz, the measurement time for each trace was 10s.

In the experiment, we examined the correlations between the two output modes EPR1 and EPR4. The various noise levels are compared with the corresponding shot noise levels and the noise levels of the individual beams. First, the noise level of the sum signal of beams EPR1 and EPR4 was measured and compared with the noise power of the individual beams, i.e. the variances of $i1$ and $i4$ and $i1 + i4$ were measured, not yet taking into account the result from the Bell-state measurement, i_{Bell}^+ . This corresponds to the case of the full entanglement swapping protocol with respect to the amplitude quadrature only without transmission of the classical information from the Bell-state measurement.

There are no correlations between the two modes EPR1 and EPR4, i.e.

$$V(\hat{X}_{\text{EPR1}} + \hat{X}_{\text{EPR4}}) = V(\hat{X}_{\text{EPR1}}) + V(\hat{X}_{\text{EPR4}}) \quad (4)$$

which can be seen on the left side of Fig. 5, and which is obvious as the two entanglement sources are independent.

The noise power of the beams EPR1 and EPR2 shows that each single beam is very noisy. This indicates that the squeezer does not generate minimum uncertainty states, but states which acquire excess phase noise of about 20dB, an effect that originates from the propagation of the light through the fiber. Although we tried to set up an exact replica of the first squeezer, the noise power of the generated EPR-beams of the second squeezer is different from that of the first squeezer.

In a second step, the correlations between EPR1 and EPR4 are checked again, this time taking into account the result of the Bell-measurement. The photocurrent of EPR4 is modified to give $i4 + i_{\text{Bell}}^+$. This photocurrent is added to $i1$. The noise power of the resulting photocurrent drops to the shot noise level of two beams, indicating that there are strong correlations between $i1$ and $i4 + i_{\text{Bell}}^+$. The noise levels are plotted on the right side of Fig. 5. This situation corresponds to the case where the classical information gained from the Bell-state measurement is transmitted and mode EPR4 is modulated and the correlations between OUT1 and OUT2 are measured (compare Fig. 1). This result clearly indicates that the full entanglement swapping experiment should be possible. With the given squeezing values, a squeezing variance $V_{\text{sq}}^+(\delta\hat{X}) = 1$ is expected for the output modes. The limitation in the experiment so far is the relatively low detected input squeezing of 3dB, otherwise correlations below the shot noise level would be visible. However, there is the 3dB penalty due to the fact that the squeezed states used have a high degree of excess phase noise. The relatively low resulting squeezing values are partly caused by the detection scheme, where at least three detectors were involved in the measurement of each individual noise

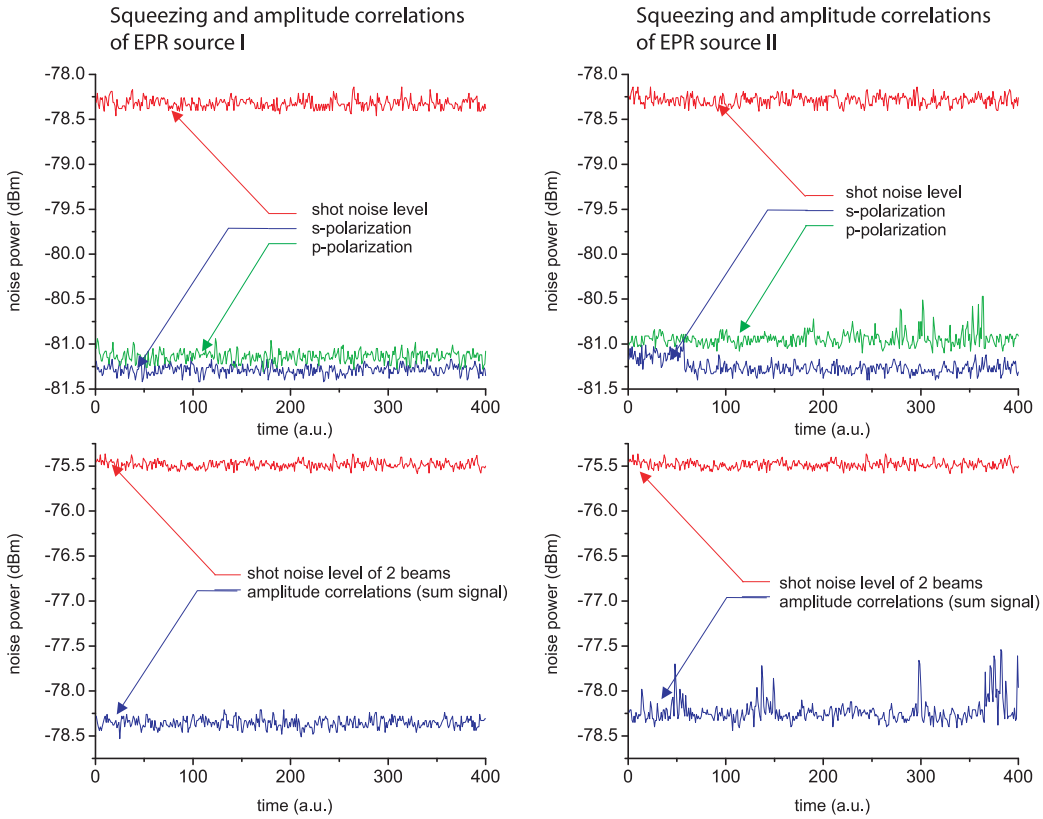


FIG. 4: Characterization of the two entanglement sources: The pictures on the top show the amplitude noise for s- and p-polarization, while the pictures at the bottom show the sum-signal of the EPR-entangled beams. In all graphs, the corresponding shot noise level is depicted. Each curve consists of 400 measurement points over a time period of 10sec. The measured noise traces are not corrected for the electronic noise which was at -87.8dBm .

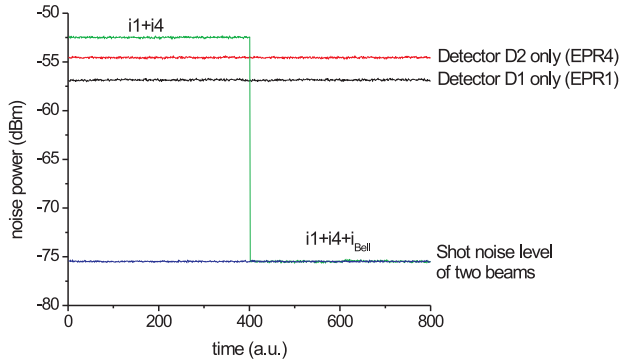


FIG. 5: Noise power of different combinations of the output modes: Traces of the single beams EPR1 and EPR4 are shown together with the combined shot noise level of two beams. On the left side, the sum signal of EPR1 and EPR4 is detected, on the right side, the signal from the Bell-measurement is added to the photocurrent detected on mode EPR4. The signal trace incidently coincides with the shot noise level of two beams. Each part of the trace (left and right) consists of 400 measurement points over a time period of 10s. The measured noise traces are not corrected for the electronic noise which was at -87.8dBm .

trace, which causes some balancing problems of the electronics.

Although the squeezing variance expected in the full experiment is at the shot noise limit, there are hints that the teleportation of a highly non-classical state with continuous variables is possible. We can speak of successful quantum teleportation of beam EPR2 on beam EPR4 in the following sense: Let us compare the measurement results with those that can be obtained by classical teleportation, where the amplitude and phase fluctuations of the mode to be teleported are measured simultaneously and an independent coherent beam is modulated. Squeezing variances between OUT1 and OUT2 which are 1.77dB higher than those that were measured in our experiment are expected with the given degree of correlations of 3dB. This can be understood by a similar argumentation to that given by Furusawa et al. [2]. In classical teleportation, two extra units of vacuum are mixed into the system, one from the Bell-measurement and one from the coherent beam that is modulated.

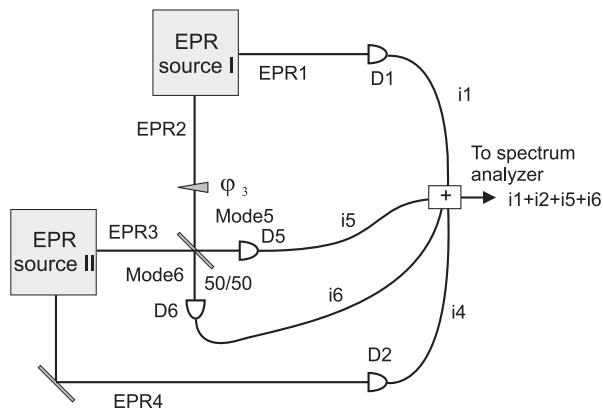


FIG. 6: Generation of a highly correlated 4-partite state

C. Interpretation of the results as multipartite correlations

Another aspect of the experiment is that the measurement results can also be interpreted in a different way. The setup is as before, two pairs of entangled beams are generated and the beams EPR2 and EPR3 are combined at a 50/50 beam splitter. We are now interested in the correlations of the complete four-mode state.

To characterize the correlations, a detector is placed in each output mode, that is in EPR1, EPR4, Mode5 and Mode6, and the photocurrents are added as depicted in Fig. 6. The situation is completely equivalent to the case where the Bell-measurement was performed and the photocurrents were added. However, the sum-photocurrent of all modes shows that the four mode state has a high degree of correlations, because the sum signal shown in Fig. 7 is 3dB below the corresponding shot noise level of four equally bright coherent states:

$$V(\hat{X}_{\text{EPR1}} + \hat{X}_{\text{Mode5}} + \hat{X}_{\text{Mode6}} + \hat{X}_{\text{EPR4}}) < 4V(\hat{X}_{\text{coh}}). \quad (5)$$

This indicates that a highly correlated four-mode state was created. The question that arises now is whether this state is genuinely four-party entangled.

A genuinely multipartite entangled state means that none of the parties is separable from any other party in the total density operator. For example, the two initial EPR sources in our setup correspond to an entangled four-mode state which is not genuinely four-party entangled. Though none of the modes is completely separable from the rest, the total state only consists of two two-party entangled states, mathematically described by the tensor product of two bright EPR states. In contrast, the output four-mode state of modes EPR1, Mode5, Mode6, and EPR4, is, in principle, a genuinely four-party entangled state, at least when assuming pure input states. This can be understood most easily by examining the corresponding four-mode Wigner function $W(\alpha_1, \alpha_5, \alpha_6, \alpha_4)$ of the output state. Assuming two pure initial EPR sources, the output state $W(\alpha_1, \alpha_5, \alpha_6, \alpha_4)$ is also pure.

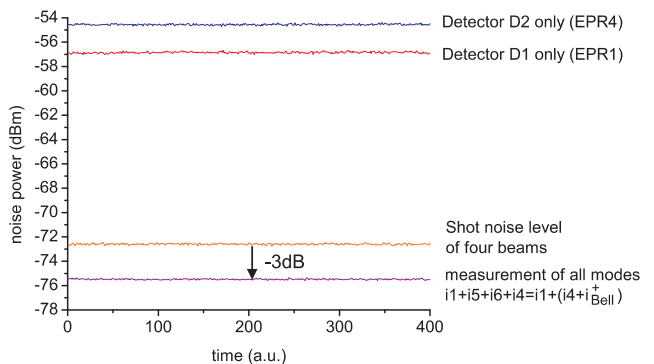


FIG. 7: Four-partite correlations: The measurement of all four modes gives a signal that is 3dB below the corresponding shot noise level. Thus the generated four-mode state is highly correlated, each individual beam having a high noise level. The measurement time was 10s. The measured noise traces are not corrected for the electronic noise which was at -87.8dBm .

For pure states, the non-factorizability of the Wigner function, $W(\alpha_1, \alpha_5, \alpha_6, \alpha_4) \neq W(\alpha_1)W(\alpha_5, \alpha_6, \alpha_4)$ and $W(\alpha_1, \alpha_5, \alpha_6, \alpha_4) \neq W(\alpha_1, \alpha_5)W(\alpha_6, \alpha_4)$ for all permutations of (1, 5, 6, 4), proves the genuine four-party entanglement. The output Wigner function for the special case of two two-mode squeezed vacuum states as the input EPR-sources is given in Ref. [25]. For any degree of the squeezing, it cannot be written in any product form hence the state is genuinely four-party entangled. Moreover, partial transposition (partial sign change of the momentum quadratures [23]) applied to its four-mode correlation matrix with respect to any possible splitting of the four modes [26, 27] always leads to an unphysical state, thus ruling out any partial separability.

The four-party correlations of the four-mode squeezed vacuum, as can be seen in the Wigner function of Ref. [25], lead to quadrature triple correlations such as $V[\hat{X}_1 - (\hat{X}_5 + \hat{X}_6)/\sqrt{2}] \rightarrow 0$ and $V[(\hat{X}_5 - \hat{X}_6)/\sqrt{2} - \hat{X}_4] \rightarrow 0$. In our experiment, due to the brightness of the beams and the direct detection scheme employed, the four-party correlations become manifest in a combination of the quadrature amplitudes of all four modes, as described by equation (5). Whether the mixedness of our entangled four-mode state due to the excess phase noise causes a significant deterioration of the four-party entanglement should be further investigated, also with respect to the experimental verification of the four-party entanglement (see below). Since the genuine four-party entanglement is present for any non-zero squeezing in the pure four-mode squeezed vacuum state [26], we expect that the mixed state in our experiment remains genuinely four party entangled.

To further characterize and describe the correlations of the four-mode state, we measured the noise of the combination of three beams, that is the variance of the photocurrents $i1 + i5 + i6 = i1 + i_{\text{Bell}}^+$ and $i5 + i6 + i4 = i_{\text{Bell}}^+ + i4$, which are plotted in Fig. 8. These signals ex-

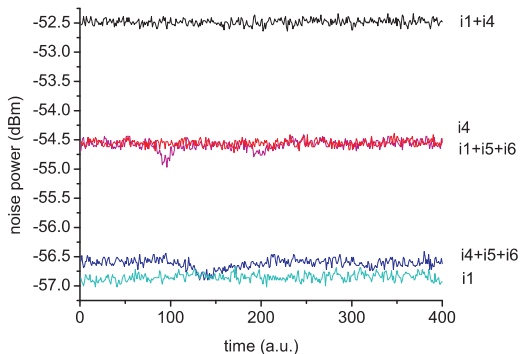


FIG. 8: Correlations of the four-mode state. Measurement of three modes compared with the noise levels of the individual beams. The measurement time was 10s. The shot noise level for three modes is about -73.7 dBm.

hibit a high noise level compared with the shot noise level. To be more precise, the noise level of $i1 + i5 + i6$ equals the noise level of $i4$ (EPR4) and $i5 + i6 + i4$ equals $i1$ (EPR1). This behaviour becomes clear by the following considerations: The sum-signal from Mode5 and Mode6, i.e. i_{Bell}^+ , contains the full amplitude fluctuations of EPR2 and EPR3. Thus by taking the sum with EPR1, only the fluctuations originating from EPR3 remain, as EPR1 and EPR2 were initially entangled and the fluctuations cancel almost completely compared with the noise of a single beam. Thus the measured noise level of $i1 + i5 + i6$ is equal to the fluctuations of beam EPR3 which has the same noise level as beam EPR4. Similarly, the noise level of the combined measurement of $i5 + i6 + i4$ can be explained. This measurement is consistent with the fact that the excess noise of the individual EPR-beams of the different EPR-sources is slightly different. As mentioned before, there are no correlations between the beams EPR1 and EPR4, as the variance of $i1 + i4$ is just the sum of the variances of $i1$ and $i4$.

IV. DISCUSSION AND OUTLOOK

A. Phase measurement: Full proof of entanglement swapping

The full proof of entanglement swapping will be more challenging as not only the correlations in the amplitude quadrature, but also those in the phase quadrature must be checked. For this purpose, a real modulation of beam EPR4 is needed. As intense entangled beams are used, no local oscillator can be employed to measure correlations in the phase quadrature due to the saturation of the detectors. Instead, some interferometric scheme is needed to measure the correlations in the phase quadrature. This can be achieved by letting the two output modes, OUT1 and OUT2, interfere at another 50/50 beam splitter.

Two possible interferometric detection schemes will be described to test whether a pair of beams, here called

EPR1 and EPR2, coming from a black box are entangled or not. In the first case, the noise power can be measured in one of the output ports of the interferometer using balanced detection (compare Fig. 9a). When the correlations in the amplitude quadratures of EPR1 and EPR2 have already been measured, correlations in the phase quadrature can be determined from an amplitude quadrature measurement of OUT1 or OUT2. If squeezing occurs, then also the phase quadrature is correlated and the beams EPR1 and EPR2 must be entangled [21]. It is also possible to check directly if the outgoing beams are non-separable: The variance of the sum photocurrent measured at the output of the interferometer is proportional to the sum of the squeezing variances, see Eq.(3). Thus the Duan non-separability criterion can be verified in a single measurement [24]. It was shown that, if squeezing occurs for a certain interference phase θ , the states EPR1 and EPR2 are necessarily entangled [24], a consequence of the non-separability criterion for continuous variables.

The other possibility is to put a detector in each output port and record the sum and the difference of the photocurrents (see Fig. 9b). The difference signal is proportional to the variance $V(\hat{Y}_{\text{EPR1}} - \hat{Y}_{\text{EPR2}})$ which drops below the shot noise level if there are non-classical correlations in the phase quadrature. The correlations in the amplitude quadrature can be checked simultaneously by taking the sum of the photocurrents. This measurement is of the same type as the Bell-state measurement in the entanglement swapping process. This detection scheme is also used for dense coding experiments [1] and was proposed for a continuous variable entanglement swapping experiment [28].

Alternatively, phase detection $\delta\hat{Y}_{\text{OUT1}}$ and $\delta\hat{Y}_{\text{OUT2}}$ can be performed on beams OUT1 and OUT2 respectively. For this purpose, an extremely unbalanced interferometer can be used [29], which maps phase fluctuations onto amplitude fluctuations for certain measurement frequencies. At the repetition rate of 82MHz of our laser system, an arm length difference of about 7.2m is required to measure phase fluctuations at a radio frequency of 20.5MHz. In that case, a phase shift is accumulated which leads to a 90° rotation of the quantum uncertainty sideband. After interference and together with the detection scheme, the phase noise of the input beam can be recorded in direct detection (see Fig. 10). Thus the phase shift for the rf-signal has to be adjusted as well as the optical interference phase such that the two output ports are equally intense. With such an interferometer, it will be possible to avoid phase modulation, as in the case of the amplitude fluctuations, and check directly the obtained photocurrents from the phase measurement together with the photocurrent from the Bell-measurement i_{Bell}^- for non-classical correlations.

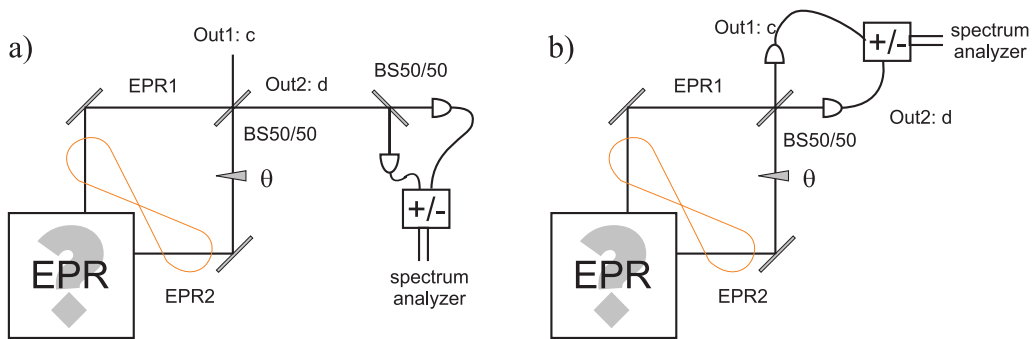


FIG. 9: Two possible setups for an indirect measurement of correlations in the phase quadrature of two beams EPR1 and EPR2. Both input beams are superimposed on a 50/50 beam splitter. In a) the noise variance of one output port is detected. This also provides a direct measure for the non-separability of states EPR1 and EPR2. In b) the signal from both output ports is detected and the difference channel provides information about the correlations of the phase quadrature of the beams EPR1 and EPR2.

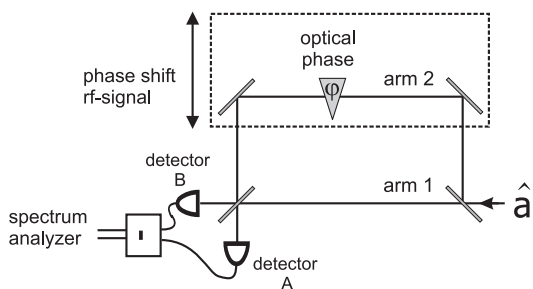


FIG. 10: Unbalanced interferometer for detection of phase fluctuation without local oscillator.

B. Criteria for multipartite entanglement

The four-party correlated state generated by the interference of two two-party entanglement sources could be an important requisite for multipartite quantum communication and networking. However, it should be first verified experimentally that the generated state is indeed genuinely four-party entangled. For Gaussian states, the full characterization of multipartite entangled states requires the detection of all independent entries of the correlation matrix. However, in Ref. [26], inequalities are derived which impose necessary conditions onto a multi-party multi-mode state to be partially or fully separable. Hence violations of these conditions rule out any form of separability, thus being sufficient for genuine multipartite entanglement. These criteria involve measurements of linear combinations for the two conjugate quadratures of all modes. The conditions are expressed in terms of the sum of the variances of these combinations. This is similar to the Duan criterion stated in equation (3), where the sum of the squeezing variances of the \hat{X} and \hat{Y} quadratures is considered. Such criteria are only sufficient and not necessary for entanglement, but they apply to arbitrary quantum states (pure, mixed, Gaussian, or non-Gaussian). By using criteria based on quadrature linear combinations for the verification of genuine multipartite

entanglement, the measurement of the entire correlation matrix of a Gaussian state is no longer needed. However, in general, these criteria cannot be readily applied to direct detection schemes. Hence simple experimental criteria and measurement techniques like those described above for the two-mode case still have to be developed for the multi-mode case.

V. CONCLUSIONS

To summarize, we have adapted a scheme to perform entanglement swapping with intense, pulsed, quadrature entangled beams using direct detection. By substituting the required optical modulation with an adapted detection setup we have shown experimentally that the amplitude correlations behave as they should for entanglement swapping. This is a strong hint for entanglement between the two output states, which have never interacted directly. To fully prove entanglement, the phase correlation still has to be measured. The joint analysis of the four individual modes shows that we have generated and partly characterized a novel four partite continuous-variable state that exhibits four-fold correlations below shot noise in the amplitude quadrature. Although so far there is no experimental proof that this state is really four-party entangled, the measured correlations support this conjecture. We have taken an experimental step towards entanglement swapping with continuous variables and produced an intense light state showing four-fold quantum correlations which is consistent with genuine four-party entanglement.

Acknowledgments

This work was supported by the Schwerpunkt Programm 1078 of the Deutsche Forschungsgemeinschaft and by the EU grant under QIPC, project IST-1999-13071 (QUICOV). The authors thank M. Langer and T. Lang

for the help with the detector electronics and J. Trautner for useful discussions about the phase measuring interferometer. Qing Pan gratefully acknowledges financial

support from China Scholarship Council.

-
- [1] X. Li, Q. Pan, J. Jing, J. Zhang, C. Xie, and K. Peng, *Phys. Rev. Lett.* **88**, 047904 (2002).
- [2] A. Furusawa, J. Sorensen, S. Braunstein, C. Fuchs, H. Kimble, and E. Polzik, *Science* **282**, 706 (1998).
- [3] D. Bouwmeester, J. W. Pan, K. Mattle, M. Eibl, H. Weinfurter, and A. Zeilinger, *Nature* **390**, 575 (1997).
- [4] C. Bennett, G. Brassard, C. Crpeau, R. Jozsa, A. Peres, and W. Wootters, *Phys. Rev. Lett.* **70**, 1895 (1993).
- [5] J. W. Pan, D. Bouwmeester, H. Weinfurter, and A. Zeilinger, *Phys. Rev. Lett.* **80**, 3891 (1998).
- [6] Y. H. Kim, S. P. Kulik, and Y. Shih, *Phys. Rev. Lett.* **86**, 1370 (2001).
- [7] I. Marcikic, H. d. Riedmatten, W. Tittel, H. Zbinden, and N. Gisin, *Nature* **421**, 509 (2003).
- [8] S. L. Braunstein and H. J. Kimble, *Phys. Rev. Lett.* **80**, 869 (1998).
- [9] T. C. Zhang, K. W. Goh, C. W. Chou, P. Lodahl, and H. J. Kimble, *Phys. Rev. A* **67**, 033802 (2003).
- [10] W. P. Bowen, N. Treps, B. C. Buchler, R. Schnabel, T. C. Ralph, H. A. Bachor, T. Symul, and P. K. Lam, *Phys. Rev. A* **67**, 032302 (2003).
- [11] H. J. Briegel, W. Dur, J. I. Cirac, and P. Zoller, *Phys. Rev. Lett.* **81**, 5932 (1998).
- [12] P. van Loock and S. L. Braunstein, *Phys. Rev. Lett.* **87**, 247901 (2001).
- [13] M. Hillery, V. Buzek, and A. Berthiaume, *Phys. Rev. A* **59**, 1829 (1999).
- [14] D. F. Walls and G. J. Milburn, *Quantum Optics* (Springer Verlag Berlin, Heidelberg, 1994).
- [15] N. Korolkova, C. Silberhorn, O. Weiß, and G. Leuchs, in *Cybernetics and Systems 2000*, edited by R. Trappl (Austrian Society for Cybernetics Studies, Vienna, 2000), p. 153.
- [16] G. Leuchs, T. Ralph, C. Silberhorn, and N. Korolkova, *J. Mod. Opt.* **46**, 1927 (1999).
- [17] J. Zhang and K. Peng, *Phys. Rev. A* **62**, 064302 (2000).
- [18] P. van Loock and S. Braunstein, *Phys. Rev. A* **61**, 010302 (1999).
- [19] S. Schmitt, J. Ficker, M. Wolff, F. König, A. Sizmman, and G. Leuchs, *Phys. Rev. Lett.* **81**, 2446 (1998).
- [20] N. Korolkova, G. Leuchs, S. Schmitt, C. Silberhorn, A. Sizmman, M. Stratmann, O. Weiß, and H.-A. Bachor, *Nonlinear Optics* **24**, 223 (2000).
- [21] C. Silberhorn, P. K. Lam, O. Weiß, F. König, N. Korolkova, and G. Leuchs, *Phys. Rev. Lett.* **86**, 4267 (2001).
- [22] L. Duan, G. Giedke, J. Cirac, and P. Zoller, *Phys. Rev. Lett.* **84**, 2722 (2000).
- [23] R. Simon, *Phys. Rev. Lett.* **84**, 2726 (2000).
- [24] N. Korolkova, C. Silberhorn, O. Glöckl, S. Lorenz, C. Marquardt, and G. Leuchs, *Eur. Phys. J. D* **18**, 229 (2002).
- [25] P. van Loock, *Fortschr. Phys.* **50**, 1177 (2002).
- [26] P. van Loock and A. Furusawa (quant-ph/0212052v1).
- [27] G. Giedke, B. Kraus, M. Lewenstein, and J. I. Cirac, *Phys. Rev. A* **64**, 052303 (2001).
- [28] J. Zhang, C. D. Xie, and K. C. Peng, *Phys. Lett. A* **299**, 427 (2002).
- [29] J. Trautner, R. Dorn, H. Telle, and G. Leuchs, Annual Report, Universität Erlangen-Nürnberg, Lehrstuhl für Optik p. 44 (1997).